

1 First passage time statistics of Brownian motion with
 2 purely time dependent drift and diffusion

3 A. Molini^{a,b,*}, P. Talkner^c, G. G. Katul^{b,a}, A. Porporato^{a,b}

4 ^a*Department of Civil and Environmental Engineering, Pratt School of Engineering, Duke*
 5 *University, Durham, North Carolina, USA*

6 ^b*Nicholas School of the Environment, Duke University, Durham, North Carolina, USA*

7 ^c*Institut für Physik, Universität Augsburg, Augsburg, Germany*

8 **Abstract**

9 Systems where resource availability approaches a critical threshold are com-
 10 mon to many engineering and scientific applications and often necessitate
 11 the estimation of first passage time statistics of a Brownian motion (Bm)
 12 driven by time-dependent drift and diffusion coefficients. Modeling such sys-
 13 tems requires solving the associated Fokker-Planck equation subject to an
 14 absorbing barrier. Transitional probabilities are derived via the method of
 15 images, whose applicability to time dependent problems is shown to be lim-
 16 ited to state-independent drift and diffusion coefficients that only depend on
 17 time and are proportional to each other. First passage time statistics, such
 18 as the survival probabilities and first passage time densities are obtained
 19 analytically. The analysis includes the study of different functional forms of
 20 the time dependent drift and diffusion, including power-law time dependence
 21 and different periodic drivers. As a case study of these theoretical results,
 22 a stochastic model of water resources availability in snowmelt dominated re-
 23 gions is presented, where both temperature effects and snow-precipitation
 24 input are incorporated.

*Corresponding author
 Preprint submitted to *Physica A*
 Email address: annalisa.molini@duke.edu (A. Molini)

25 *Keywords:* Brownian motion, Time-dependent drift and diffusion,
26 Absorbing barrier, Snowmelt

27 **1. Introduction**

28 A wide range of geophysical and environmental processes occur under
29 the influence of an external time-dependent and random forcing. Climate-
30 driven phenomena, such as plant productivity (Ehleringer et al., 1997), steno-
31 thermal populations dynamics (McClanahan & Maina, 2003), crop produc-
32 tion (Rosenzweig & Parry, 1994), the alternation between snow-storage and
33 melting in mountain regions (Hamlet & Lettenmaier, 1999; Marks et al.,
34 1998), the life cycle of tidal communities (Barranguet et al., 1998; Bertness
35 & Leonard, 1997; Charles & Dukes, 2009), and water-borne diseases out-
36 breaks (Pascual et al., 2002; Patz et al., 2005) offer a few such examples. In
37 particular, several environmental systems can be described by state variables
38 representing the availability of a resource whose dynamics is forced by diverse
39 environmental factors and climatic oscillations. Elevated regions water avail-
40 ability – mainly originating from the melting of snow masses accumulated
41 during the winter period (under the forcing of increasing temperatures), and
42 precipitation (moving from the solid precipitation to the rainfall regime) –
43 offers a relevant case study (presented in Section 4). All of these processes
44 are now receiving increased attention in several branches of ecology, climate
45 sciences and hydrology, due to their inherent sensitivity to climatic variabil-
46 ity.

47 Analogous dynamical patterns can be found in slowly-driven, non-equili-
48 brium systems with self organized criticality (*SOC*), where the density of

49 potentially relaxable sites in the system can be described via a random
50 walk with time-dependent drift and diffusion terms (Adami, 1995; Bak &
51 Paczuski, 1995; Jensen, 1998). In these systems, the time dependence in the
52 diffusion term derives from a gradual decrease of susceptible sites, so that
53 sites availability acts on the directionality and pathways (drift term) of the
54 “avalanches” till diffusion “kills” all the activity in the system (Redner, 2001,
55 pp. 120–131). Similar dynamics occur in systems displaying stochastic reso-
56 nance, where noise becomes modulated by an external periodic forcing (see
57 Bulsara et al., 1994, 1995; Gammaitoni et al., 1998; McDonnell et al., 2008,
58 and references therein).

59 In many instances, the above mentioned processes are restricted to the
60 positive semi-plane or to the time at which a certain critical threshold is
61 reached, and are represented by a Fokker-Planck (FP) equation with an ab-
62 sorbing barrier. The main focus here is on the first passage time statistics
63 of the process, such as the survival probabilities and the first passage time
64 densities. In the following, a brief review of the general properties of the
65 time-dependent drift and diffusion processes with an absorbing barrier is pre-
66 sented. For constant drift and diffusion, the conditional probabilities are usu-
67 ally obtained via the method of images due to Lord Kelvin (see Feller, 1971,
68 p. 340). The applicability of this method to the solution of time-dependent
69 problems and its limitations are discussed and a necessary and sufficient cri-
70 terion is formulated in Section 2.2. The analysis is then extended to different
71 functional forms of the time-dependent drift and diffusion terms. Section 3.1
72 shows the analytical results for the first passage time statistics for a power-law
73 time dependent drift and diffusion, while time-periodic drivers are analyzed

74 in Section 3.2 (see Jung, 1993; Kim et al., 2010; Talkner et al., 2005, and
75 references therein, for a more comprehensive review of periodically-driven
76 stochastic processes). Finally, in Section 4, we present a stochastic model of
77 the total mountain water equivalent during the apex phase of the melting
78 season, incorporating both temperature effects and snow-precipitation input
79 in the form of a power-law time-dependent Bm with an absorbing boundary.

80 2. Modeling Framework

81 When a time-dependent random forcing is the dominant driver of the dy-
82 namics, a general representation for the state variable $x(t)$ can be formulated
83 in the form of a stochastic differential equation given by

$$dx(t) = \mu(t) dt + \sigma(t) dW(t) \quad (1)$$

84 where $\mu(t)$ and $\sigma(t)$ are purely time-dependent drift and diffusion terms,
85 and $W(t)$ is a Wiener process with independent and identically Gaussian
86 distributed (iid) increments $W(t) - W(s) \sim \mathcal{N}(0, t - s)$ for all $t \geq s \geq 0$. By
87 assuming $t_0 = 0$, the solution of (1) takes the form

$$x(t) = x_0 + \int_0^t \mu(s) ds + \int_0^t [\sigma(s) dW(s)] \quad (2)$$

88 where t is time and $x_0 = x(0)$ can be either a random or a non-random
89 initial condition independent of $W(t) - W(0)$. The associated FP equation
90 describing the evolution of the probability density function (pdf) of $x(t)$ can
91 be expressed as

$$\frac{\partial p(x, t|x_0)}{\partial t} = -\mu(t) \frac{\partial p(x, t|x_0)}{\partial x} + \frac{1}{2} \sigma^2(t) \frac{\partial^2 p(x, t|x_0)}{\partial x^2}, \quad (3)$$

92 where $p(x, t|x_0)$ is the transition pdf with initial condition $\delta(x - x_0)$ at t_0 .

93 Eq. (3) can also be expressed as a continuity equation for probability

$$\frac{\partial}{\partial t}p(x, t|x_0) = -\frac{\partial}{\partial x}j(x, t|x_0), \quad (4)$$

94 where

$$j(x, t|x_0) = \mu(t)p(x, t|x_0) - \frac{1}{2}\sigma^2(t)\frac{\partial p(x, t|x_0)}{\partial x}, \quad (5)$$

95 is the probability current (or flux) and $p(x, t|x_0)$ is the conditional probability.

96 The solution of the FP equation in (3), is usually approached numerically

97 (see for e.g., Schindler et al. (2005)). Whether this equation is analytically

98 solvable for different functional forms of $\mu(t)$ and $\sigma(t)$ with an absorbing

99 boundary, and whether these solutions can be applied in the study of the

100 first passage statistics at such boundary is the main focus of this work. Case

101 studies that employ these solutions are also presented.

102 *2.1. Solution with Natural Boundaries*

103 Consider first the solution of the FP equation (3) in the unbounded

104 case. Given that the drift and diffusion coefficients depend only on time,

105 the parabolic equation (3) can still be reduced to a constant-coefficient equa-

106 tion of the form

$$\frac{\partial p(z, \tau)}{\partial \tau} = \frac{\partial^2 p(z, \tau)}{\partial z^2} \quad (6)$$

107 by transforming the original variables x and t into

$$\tau = \frac{1}{2} \int \sigma^2(t) dt + A \quad (7)$$

108 and

$$z = x - \int \mu(t) dt + B \quad (8)$$

109 where A and B are generic constants. The solution with natural boundaries
 110 is then (Polyanin, 2002) $p(z, \tau) = \frac{1}{2\sqrt{\pi\tau}} \exp\left(-\frac{z^2}{4\tau}\right)$. Hence, given the initial
 111 condition

$$p(x, 0|x_0) = \delta(x - x_0), \quad (9)$$

112 the following normalized solution for an unrestricted process, starting from
 113 x_0 , can be obtained as

$$p_u(x, t|x_0) = \frac{1}{2\sqrt{\pi S(t)}} \exp\left[-\frac{(x - x_0 - M(t))^2}{4S(t)}\right], \quad (10)$$

114 where, assuming the integrability of $\mu(t)$ and $\sigma(t)$,

$$M(t) = \int_0^t \mu(s) ds \quad (11)$$

115 and

$$S(t) = \frac{1}{2} \int_0^t \sigma^2(s) ds. \quad (12)$$

116 It should be noted that the transformation in equations (8) and (7) also
 117 applies to any boundary condition imposed at a finite position. Therefore,
 118 as will be seen, it is not directly helpful in solving first passage time problems,
 119 as in that case it would lead to a problem with *moving* absorbing boundary
 120 conditions.

121 2.2. First Passage Time Distributions

122 For a Bm process commencing at a generic position x_0 at $t = 0$, the time
 123 at which this process reaches an arbitrary threshold a for the first time (first
 124 passage time) is itself a random variable whose statistics are fundamental in
 125 many branches of science such as chemistry, neural-sciences and economet-
 126 rics. In the following, it is assumed that the process is starting at a certain

127 state $x_0 > 0$ and that it is bounded to the positive semi-axis via an absorbing
 128 barrier $x = 0$. This hypothesis does not imply any loss of generality, consid-
 129 ering that the solution of Eq. (3) with an absorbing boundary condition only
 130 depends on the distance of the initial point x_0 from the threshold, but not
 131 separately on x_0 and the threshold position. Eq. (3) is then solved with the
 132 boundary condition

$$p(0, t) = 0, \quad (13)$$

133 and the additional condition of $x = +\infty$ being a natural boundary to ensure
 134 that $j(+\infty, t | x_0) = 0$. For such a system, the survival probability $F(t | x_0)$
 135 is defined as the probability of the process trajectories not absorbed before
 136 time t , i.e.

$$F(t | x_0) = \int_0^{+\infty} p(x, t | x_0) dx \quad (14)$$

137 and the first passage probability density $g(t | x_0)$ is either the “rate of de-
 138 crease” in time of F

$$g(t | x_0) = -\frac{\partial}{\partial t} F(t | x_0) \quad (15)$$

139 or, alternatively, the negative probability current at the boundary

$$g(t | x_0) = \frac{\sigma^2(t)}{2} \frac{\partial}{\partial x} p(x, t | x_0) |_{x=0}, \quad (16)$$

140 since $p(0, t | x_0) = 0$ from (13).

141 *2.3. Method of Images in Time-Dependent Systems*

142 When the drift and diffusion terms are independent of t and x , Eq. (3)
 143 with absorbing boundaries can be readily solved by the method of images,
 144 often adopted in problems of heat conduction and diffusion (Cox & Miller,
 145 1965; Daniels, 1982; Lo et al., 2002; Redner, 2001). This method can also

146 be used for solving boundary-value problems for a Bm with particular forms
 147 of time-dependent drift and diffusion. The basic premise of this method is
 148 that given a linear PDE with a point source (or sink) subject to homogeneous
 149 boundary conditions in a finite domain, its general solution can be obtained as
 150 a superposition of many ‘free space’ solutions (i.e. disregarding the boundary
 151 conditions) for a number of virtual sources (i.e. outside the domain) selected
 152 so as to obtain the correct boundary condition. The image source (or sink)
 153 is placed as mirror image of the original source (or sink) from the boundary
 154 with a strength or intensity selected to match the boundary condition.

155 Consider equation (3) with the conditions (9) and (13). To solve this
 156 problem with the method of images, the barrier at 0 is replaced by a mirror
 157 source located at a generic point $x = y$, with $y < 0$ such that the solutions of
 158 the Fokker-Planck equation emanating from the original and mirror sources
 159 exactly compensate each other at the position of the barrier at each instant
 160 of time (Redner, 2001). This implies the initial conditions in (9) must now
 161 be modified to

$$p(x, 0) = \delta(x - x_0) - \exp(-\eta) \delta(x - y), \quad (17)$$

162 where η determines the strength of the mirror image source. Due to the lin-
 163 earity of the FP equation, the solution in the presence of the initial condition
 164 (17) is the superposition of elementary solutions

$$p(x, t|x_0) = p_u(x, t|x_0) - \exp(-\eta) p_u(x, t|y). \quad (18)$$

165 Since the condition (13) requires that $p(0, t|x_0) = 0$, one obtains that

$$\frac{(M(t) + x_0)^2}{4S(t)} = \eta + \frac{(M(t) + y)^2}{4S(t)} \quad (19)$$

166 for all $t > 0$. By assuming $t = 0$, we have $x_0^2 = y^2$ and recalling that $y < 0$,
 167 the resulting image position is $-x_0$. This, inserted again in Eq. (19), yields

$$\frac{M(t)}{S(t)} = \frac{\eta}{x_0} = q, \quad (20)$$

168 where the constant q is analogous to the Péclet number of the process – i.e.
 169 the ratio between the advection and diffusion rates (Redner, 2001).

170 After differentiating (20) with respect to t , it is seen that the method
 171 of images requires that the drift and the diffusion terms be proportional to
 172 each other. Namely, the intensity η of the image source must be constant in
 173 time. In fact, only in this case it is still possible to transform the original
 174 time scale into a new one, for which the transformed process is governed
 175 by time-independent drift and diffusion terms. Hence, writing the drift and
 176 diffusion terms as

$$\mu(t) = kh(t) \quad \text{and} \quad \frac{\sigma^2}{2} = lh(t), \quad (21)$$

177 the associated FP equation is

$$\frac{\partial p}{\partial t} = h(t) \left(-k \frac{\partial}{\partial x} + l \frac{\partial^2}{\partial x^2} \right) p. \quad (22)$$

178 Transforming the original time t variable in

$$\tilde{\tau} = \int_0^t h(s) ds \quad (23)$$

179 Equation (22) finally becomes

$$\frac{\partial p}{\partial \tilde{\tau}} = \left(-k \frac{\partial}{\partial x} + l \frac{\partial^2}{\partial x^2} \right) p. \quad (24)$$

180 This condition is valid for any time-dependent diffusion when the drift is
 181 identically vanishing. Assuming the proportionality in (20) between $\mu(t)$

182 and $\sigma(t)$, the general solution for (3) under conditions (9) and (13) can be
 183 written as

$$p(x, t|x_0) = \frac{1}{2\sqrt{\pi S(t)}} \left\{ \exp \left[-\frac{(x-x_0-M(t))^2}{4S(t)} \right] - \exp(-x_0q) \exp \left[-\frac{(x+x_0-M(t))^2}{4S(t)} \right] \right\}, \quad (25)$$

184 provided $M(t) = qS(t)$. Substituting for constant drift and diffusion in (25)
 185 one recovers the well-known solution for a biased Bm (Cox & Miller, 1965)

$$p(x, t|x_0) = \frac{1}{\sqrt{2\pi}\sqrt{\sigma^2 t}} \left\{ \exp \left[-\frac{(x_0-x+\mu t)^2}{2\sigma^2 t} \right] - \exp \left(-\frac{2x_0\mu}{\sigma^2} \right) \exp \left[-\frac{(x+x_0-\mu t)^2}{2\sigma^2 t} \right] \right\} \quad (26)$$

186 with survival function $F(t|x_0)$ given by

$$F(t|x_0) = \Phi \left\{ \frac{\mu t + x_0}{\sigma\sqrt{t}} \right\} - \exp \left(-\frac{2x_0\mu}{\sigma^2} \right) \Phi \left\{ \frac{\mu t - x_0}{\sigma\sqrt{t}} \right\}, \quad (27)$$

187 where Φ is the standard normal integral, and first passage time distribution

$$g(t|x_0) = \frac{x_0}{\sigma\sqrt{2\pi}t^{3/2}} \exp \left[-\frac{(x_0 + \mu t)^2}{2\sigma^2 t} \right]. \quad (28)$$

188 Equation (28) is the Wald (or inverse Gaussian) density function, that for a
 189 zero drift becomes of order $t^{-3/2}$ as $t \rightarrow +\infty$ (the first passage time has no
 190 finite moments for pure diffusion).

191 Similarly, the solution to the FP in equation (3) with a reflecting bound-
 192 ary at $x = 0$ can be obtained by the method of images provided that drift
 193 and diffusion are proportional to each other. The solution then becomes

$$p(x, t|x_0) = \frac{1}{2\sqrt{\pi S(t)}} \left\{ \exp \left[-\frac{(x-x_0-M(t))^2}{4S(t)} \right] + \exp(-x_0q) \exp \left[-\frac{(x+x_0-M(t))^2}{4S(t)} \right] - \frac{1}{2} \frac{M(t)}{S(t)} \exp \left(\frac{x\eta}{x_0} \right) \left[1 - \operatorname{erf} \left(\frac{x+x_0+M(t)}{2\sqrt{S(t)}} \right) \right] \right\}, \quad (29)$$

194 with $\frac{1}{2} \left[1 - \operatorname{erf} \left(\frac{x+x_0+M(t)}{2\sqrt{S(t)}} \right) \right]$ being the Q-function representing the tail prob-
 195 ability of a Gaussian distribution. Equation (29) generalizes the solution in
 196 Cox & Miller (1965) for a Bm with constant drift and diffusion and a reflect-
 197 ing boundary at 0.

198 3. Time Dependent Drift and Diffusion

199 3.1. Power-Law Time Dependence

200 As a first example of Bm with purely time-dependent drivers, the case of
 201 an unbiased diffusion ($q = 0$) and power-law time dependent diffusion term
 202 $\sigma^2(t) = 2At^\alpha$ and $\alpha > -1$ are considered. For this process, the conditional
 203 probability $p(x, t|x_0)$ with absorbing barriers at 0, takes on the form

$$p(x, t|x_0) = \frac{\sqrt{1+\alpha}}{2\sqrt{A\pi}} t^{-(\alpha+1)} \left\{ \exp \left[-\frac{t^{-(\alpha+1)}(x-x_0)^2(1+\alpha)}{4A} \right] - \exp \left[-\frac{t^{-(\alpha+1)}(x+x_0)^2(1+\alpha)}{4A} \right] \right\}, \quad (30)$$

204 while the survival function becomes

$$F(t|x_0) = \operatorname{erf} \left(\frac{x_0(1+\alpha)^{\frac{1}{2}} t^{-\frac{\alpha+1}{2}}}{2\sqrt{A}} \right). \quad (31)$$

205 Figure 1(a) shows the conditional probability (30) at a fixed time instance $t =$
 206 15 time steps for $A = 15$, $x_0 = 50$, and $\alpha = -0.1$ (bold line) 0.5 (thin line),
 207 and 1 (dotted line). Given the asymptotic properties of the error function
 208 (Abramowitz & Stegun, 1964), the long-time behavior of $F(t|x_0)$ is then
 209 $\sim \frac{x_0(1+\alpha)^{1/2}}{2\sqrt{A}} t^{-\frac{\alpha+1}{2}}$, recovering for $\alpha = 0$ the $-1/2$ tail decay of an unbiased
 210 constant diffusion (see Figure 1(b)). Also, by differentiating Eq. (31), one
 211 obtains

$$g(t|x_0) = \frac{x_0}{2\sqrt{\frac{A\pi}{(\alpha+1)^3}} t^{(3+\alpha)/2}} \exp \left[-\frac{x_0(\alpha+1)t^{-(\alpha+1)}}{4A} \right] \quad (32)$$

212 whose tail behaves as $\sim t^{-\left(\frac{3+\alpha}{2}\right)}$. Hence, Eq. (32) is an inverse Gaussian
 213 distribution – that for $\alpha = 0$ becomes an inverse Gamma distribution with
 214 shape parameter $1/2$ (Johnson et al., 1994, pp. 284–285). These solutions
 215 characterize inter-arrival times between intermittent events when a system
 216 displays sporadic randomness (Gaspard & Wang, 1988; Molini et al., 2009;
 217 Rigby & Porporato, 2010).

218 The solutions in the case of proportional power-law diffusion and drift can
 219 be derived in an analogous manner. For $\mu(t) = qAt^\alpha$ and $\sigma(t) = \sqrt{2}A^{1/2}t^{\alpha/2}$,
 220 the conditional probability $p(x, t|x_0)$ takes the form

$$\begin{aligned}
 p(x, t|x_0) = & \\
 & \frac{\sqrt{\alpha+1}t^{-(\alpha+1)/2}}{2\sqrt{A\pi}} \left\{ \exp \left[-\frac{(1+\alpha)t^{-(\alpha+1)} \left(-x + \frac{Aqt^{1+\alpha}}{1+\alpha} + x_0 \right)^2}{4A} \right] \right. \\
 & \left. - \exp \left[-qx_0 - \frac{(1+\alpha)t^{-(\alpha+1)} \left(x - \frac{Aqt^{1+\alpha}}{1+\alpha} + x_0 \right)^2}{4A} \right] \right\} \quad (33)
 \end{aligned}$$

221 and the survival function, now incorporating the drift contribution, can be
 222 written as

$$\begin{aligned}
 F(t|x_0) = & \Phi \left\{ t^{-\frac{(\alpha+1)}{2}} \frac{(Aqt^{\alpha+1} + x_0 + x_0\alpha)}{2\sqrt{A(\alpha+1)}} \right\} \\
 & - \exp(-qx_0) \Phi \left\{ t^{-\frac{(\alpha+1)}{2}} \frac{(Aqt^{\alpha+1} - x_0 - x_0\alpha)}{2\sqrt{A(\alpha+1)}} \right\}. \quad (34)
 \end{aligned}$$

223 For positive q 's, $F(t|x_0)$ tends in the long term to $1 - \exp(-qx_0)$, while for
 224 negative q 's, $F(x, t|x_0) \sim \frac{2\sqrt{\alpha+1}}{q\sqrt{A}} t^{-\frac{\alpha+1}{2}} \exp\left(-\frac{q\sqrt{A}t^{\frac{\alpha+1}{2}}}{2\sqrt{\alpha+1}}\right)$. This fact implies
 225 that the probability for a trajectory to be eventually absorbed is 1 for the
 226 biased process directed towards the barrier, and $\exp(-qx_0)$ when the bias is
 227 away from the barrier (infinite aging). When the state variable represents
 228 the availability of a resource in time, the sign of q determines if this resource

229 is subject to continuous accumulation (positive q), or it undergoes a total
 230 depletion (negative q) with probability 1. Such a result is analogous to the
 231 one of a simple biased Bm with constant drift and diffusion (Redner, 2001),
 232 with the difference that in this case, $F(t|x_0)$ decays to 0 or $1 - \exp(-qx_0)$
 233 with a rate that is governed by α .

234 As an example, Figures 1 (c) and (d) respectively show a negatively biased
 235 power-law time-dependent Bm and a positively biased one for the same set
 236 of parameters in (b) and $q = -0.1$ and $q = 0.1$, for $A = 1$, $x_0 = 1$ and $\alpha = 0$
 237 (constant diffusion, bold line), -0.5 (thin dotted line), 0.5 (dashed line), and
 238 1 (thin line). As evident in panel (c), $F(x, t|x_0)$ presents a faster decay to
 239 zero with increasing α , while for the positively biased Bm in panel (d) the
 240 decay to the asymptotic value $1 - \exp(-qx_0)$ is slower with decreasing α .

241 Finally, $g(t|x_0)$ can be obtained from (34) as

$$g(t|x_0) = \frac{x_0(1+\alpha)^{3/2}}{2\sqrt{\pi A}t^{\frac{3+\alpha}{2}}} \exp\left[-\frac{t^{-(\alpha+1)}(Aqt^{\alpha+1} + x_0 + \alpha x_0)^2}{4A(1+\alpha)}\right] \quad (35)$$

242 where for $\alpha = 0$ the decay of $g(t|x_0)$ recovers the constant diffusion $t^{-3/2}$ -law
 243 for $t \rightarrow \infty$ and $q = 0$.

244 3.2. Periodic Drift and Diffusion

245 In this section, the case of a periodic diffusion in the form $\sigma^2(t) =$
 246 $[2A \cos(\omega t)]^2$ and $q = 0$ is considered. For periodically driven diffusion, the
 247 conditional probability can be derived in the form

$$p(x, t|x_0) = \left(\frac{\omega}{\pi\vartheta(t)}\right)^{\frac{1}{2}} \exp\left[-\frac{2\omega(x^2+x_0)}{\vartheta(t)}\right] \left\{ \exp\left[\frac{\omega(x+x_0)^2}{\vartheta(t)}\right] - \exp\left[\frac{\omega(x-x_0)^2}{\vartheta(t)}\right] \right\} \quad (36)$$

248 where $\vartheta(t) = A^2[2\omega t + \sin(2\omega t)] > 0$. Thus, the solution becomes modulated
 249 in time with frequency ω . The survival probability is in turn

$$F(t|x_0) = \operatorname{erf} \left(x_0 \sqrt{\frac{\omega}{\vartheta(t)}} \right), \quad (37)$$

250 that is represented in Figure 2 for different values of the frequency ω . Finally,
 251 the first passage time density is an ω -modulated inverse Gaussian distribution

$$g(t|x_0) = \frac{4x_0 A^2 \omega^{3/2} \cos(\omega t)^2}{\sqrt{\pi}} \frac{\exp \left(-\frac{\omega x_0^2}{\vartheta(t)} \right)}{\vartheta(t)^{3/2}}. \quad (38)$$

252 In the case $q \neq 0$, the conditional probability $p(x, t|x_0)$ becomes

$$p(x, t|x_0) = \frac{\sqrt{\omega}}{\sqrt{\pi q \vartheta(t)}} \left\{ \exp \left[-\frac{\omega \left(x_0 - x + \frac{q\vartheta(t)}{4\omega} \right)^2}{\vartheta(t)} \right] - \exp \left[-qx_0 - \frac{\omega \left(x_0 + x - \frac{q\vartheta(t)}{4\omega} \right)^2}{\vartheta(t)} \right] \right\}, \quad (39)$$

253 where, again, the absorption at the barrier represents a recurrent ($q < 0$) or a
 254 transient ($q > 0$) state, as was observed for the power-law drift and diffusion
 255 process in Section 3.1. The recurrent case is illustrated in Figure 3 (b)-
 256 (d), where we report the time-position evolution of $p(x, t|x_0)$ as a function of
 257 increasing ω . From (39), given $\frac{\omega}{\vartheta} > 0$, the expression for the survival function
 258 can be derived and takes the form

$$F(t|x_0) = \frac{1}{2} \left[1 + \operatorname{erf} \left(\frac{q\vartheta(t) + 4x_0\omega}{4\sqrt{\omega\vartheta(t)}} \right) + \exp(-qx_0) \operatorname{erfc} \left(\frac{q\vartheta(t) - 4x_0\omega}{4\sqrt{\omega\vartheta(t)}} \right) - 2 \exp(-qx_0) \right], \quad (40)$$

259 which, given the equality $\operatorname{erfc}(-x) = 2 - \operatorname{erfc}(x)$, can be alternatively ex-
 260 pressed as

$$F(t|x_0) = \Phi \left\{ \frac{q\vartheta(t) + 4x_0\omega}{2\sqrt{2\omega\vartheta(t)}} \right\} - \exp(-qx_0) \Phi \left\{ \frac{q\vartheta(t) - 4x_0\omega}{2\sqrt{2\omega\vartheta(t)}} \right\}. \quad (41)$$

261 The first passage time density $g(t|x_0)$ is given by

$$g(t|x_0) = \frac{4A^2x_0\omega^{3/2}\cos(\omega t)^2}{\sqrt{\pi}\vartheta(t)^{3/2}} \exp\left[-\frac{(q\vartheta(t)+4x_0\omega)^2}{16\omega\vartheta(t)}\right]. \quad (42)$$

262 The method of images can also be applied to the solution of different
 263 forms of periodic drivers, such as the case $\mu(t) = q(B + A\cos(\omega t))$ and
 264 $\sigma(t) = \sqrt{2(B + A\cos(\omega t))}$, with $(B + A\cos(\omega t)) > 0$. In this last case, the
 265 drift term is the same as the one usually investigated in neuron dynamics
 266 by simple integrate-and-fire models displaying stochastic resonance (see for
 267 example the neuron dynamics case in Bulsara et al., 1994, 1995). In those
 268 models, the diffusion is usually constant so that the condition in equation
 269 (20) is not satisfied. Thus, it is often implied that $\mu(t) \ll \sigma^2/2$ to approxi-
 270 mately resemble a time dependent diffusion with drift identically vanishing or
 271 that $B \gg A$ (approximating the simpler constant drift and diffusion case).
 272 In these cases, the method of images only offers approximated solutions (Bul-
 273 sara et al., 1994, 1995)). Specifically, for a time dependent (and periodic)
 274 drift $\mu(t) = B + A\cos(\omega t)$ and constant diffusion $\frac{1}{2}\sigma^2$, an approximation for
 275 $p(x, t|x_0)$ in the presence of an absorbing barrier at 0 can still be obtained by
 276 using the method of images conditional to the fact that $\mu(t) \ll \sigma^2/2$. Only
 277 by adopting this assumption in fact, we can obtain an (approximated) solu-
 278 tion for the survival function by means of Eq. 25 although drift and diffusion
 279 are not strictly proportional to each other. In this way we find

$$F(t|x_0) = \frac{1}{2} \left\{ \operatorname{erfc}\left(\frac{Bt + \frac{A\sin(\omega t)}{\omega} - x_0}{\sqrt{2\sigma\sqrt{t}}}\right) - \exp\left[\frac{2x_0(B\omega t + A\sin(\omega t))}{\sigma^2\omega t}\right] \operatorname{erfc}\left(\frac{Bt + \frac{A\sin(\omega t)}{\omega} + x_0}{\sqrt{2\sigma\omega\sqrt{t}}}\right) \right\} \quad (43)$$

280 and, analogous to Bulsara et al. (1994), from equation (15) the first passage

281 density can be expressed as

$$\begin{aligned}
g(t|x_0) = & \frac{x_0 \exp\left\{-\frac{[Bt + \frac{A\sin(\omega t)}{\omega} - x_0]^2}{2\sigma^2 t}\right\}}{\sqrt{2\pi\sigma t^{\frac{3}{2}}}} \\
& + \frac{A \exp\left\{\frac{[(x_0 + Bt)\omega + A\sin(\omega t)]^2}{2\sigma^2 \omega^2 t}\right\} \operatorname{erfc}\left(\frac{Bt + \frac{A\sin(\omega t)}{\omega} + x_0}{\sqrt{2\sigma\sqrt{t}}}\right) \left[t \cos(\omega t) - \frac{1}{\omega} \sin(t\omega)\right]}{\sigma^2 t^2}
\end{aligned} \tag{44}$$

282 The approximated nature of the solution is evidenced by the fact that, the
283 image source intensity is no longer constant in time, so that by evaluating
284 the probability current in 0 we obtain

$$\tilde{g}(t|x_0) = \frac{x_0}{\sqrt{2\pi\sigma t^{3/2}}} \exp\left\{-\frac{[\omega(Bt - x_0) + A\sin(\omega t)]^2}{2\omega^2 \sigma^2 t}\right\}, \tag{45}$$

285 which is different from (44). In any case, the first passage time pdf in equa-
286 tion (44) is in good agreement with the numerical simulations in Bulsara
287 et al. (1994, 1995). Also, when $A \rightarrow 0$ both the (44) and the (45) tend to
288 the first passage time pdf for a simple biased Bm.

289 As highlighted in Figure (4), when the magnitude of $\mu(t)$ becomes sig-
290 nificant, the two pdfs diverge due to the losses of probability density at the
291 barrier (Eq. (45)). For this reason, the method of images cannot be con-
292 sidered a general approach to solving problems described by Eq. (3) with a
293 time-dependent Péclet number.

294 4. A Case Study: Snowmelt Dynamics

295 Snowmelt represents one of the paramount sources of freshwater for many
296 regions of the world, and is sensitive to both temperature and precipitation
297 fluctuations (Barnett et al., 2004, 2005; Barnett & Pierce, 2009; Pepin &
298 Lundquist, 2008; Perona et al., 2001; You et al., 2010). Snow dynamics is

299 characterized by an accumulation phase during which snow water equivalent
300 (i.e. the amount of liquid water potentially available by totally and instant-
301 neously melting the entire snowpack) increases until a seasonal maximum h_0
302 is reached, followed by a depletion phase in which the snow mantel gradually
303 decays (and releases the stored water content) due to the increasing air tem-
304 perature. Such a dynamics is complex and its general description requires
305 numerous physical parameters that are rarely measured or available. In this
306 section, we focus on a stochastic model describing the total water equivalent
307 from both snow and rainfall during the melting season, as forced/fed by both
308 precipitation (moving from the solid to the liquid precipitation regime) and
309 increasing air temperature.

310 Due to the simplified nature of our stochastic model, we will consider
311 the total potential water availability (in terms of water equivalent) as the
312 key variable, thus neglecting any further effects connected with snow per-
313 colation and metamorphism (De Walle & Rango, 2008). Snowfalls are here
314 assumed to become more sporadic progressing into the warm season and the
315 predominant controls over fresh water availability during the melting period
316 are increasing air temperature and liquid precipitation. Accordingly, the
317 melting phase is described by a power-law time dependent drift directed to-
318 wards the total depletion of the snow mantle and by a power-law diffusion
319 whose positive and negative excursions represent respectively precipitation
320 events and pure melting periods. The melting process is often described by
321 a linear function of time by using the so called “degree-day” approach with
322 time-varying melting-rate coefficients (De Walle & Rango, 2008). Consid-
323 ering that temperature varies seasonally and increases during the melting

324 season, a power-law form for drift and diffusion during the spring season,
 325 still represents a parametrically-parsimonious and effective approximation of
 326 the basic driver of the process.

327 Under these assumptions, the dynamics of the total water equivalent
 328 depth for unit of area h – i.e. the amount of fresh water potentially available
 329 from both snow accumulation and rainfall (Bras, 1990) – at a given point in
 330 space can be reasonably described by the Langevin equation

$$dh = -qkt^\alpha dt + \sqrt{2kt^\alpha}dW(t) \quad (46)$$

331 where k (with dimension $L^2/T^{\alpha+1}$) represents the accumulation/ablation
 332 rate. Note that here h includes both the rainfall and snowmelt contribu-
 333 tions. Also, we hypothesize that both the drift and the diffusion scale with
 334 the same exponent α . This is a reasonable assumption given that variability
 335 of the process is expected to increase proceeding into the warm season. The
 336 initial condition is given by the snow water equivalent (*SWE*) h_0 , accumu-
 337 lated during the cold season. The survival probability $F(t|h_0)$ for a given
 338 initial *SWE* and the first passage time density $g(t|h_0)$ can be respectively
 339 calculated from (34) and (35). Figure 5 shows few sample trajectories of
 340 the process (panel (a)) obtained by the numerical simulation of Eq. (46)
 341 by means of a forward Euler algorithm with a time step of 10^{-2} days. The
 342 conditional probability $p(h, t|h_0)$ at different instants, the first passage time
 343 density $g(t|h_0)$, and the survival function $F(t|h_0)$, for the case $\alpha = 0.25$ and
 344 $k = 0.24 \text{ mm}^2/\text{days}^\alpha$ are also shown in panels (b) to (d). Here, we calibrated
 345 the parameters to obtain the mode of the first passage time at about 40 days
 346 after reaching the maximum *SWE* of the season h_0 . The first passage time
 347 statistics presented offer important clues about the timing between melting

348 and summer fresh-water availability under different climatic scenarios (con-
349 sider for example the FPT pdf in Figure 5(c)).

350 5. Conclusions

351 The first passage time properties of Brownian motion with purely time
352 dependent drift and diffusion coefficients subjected to an absorbing barrier
353 were investigated. These processes can be used to mimic a variety of en-
354 vironmental and geophysical phenomena, representing the availability of a
355 resource and its dynamics in time (e.g. the ablation phase of a snow mass
356 accumulated during the winter period and forced by temperature and precip-
357 itation). Survival functions and pdfs for the first passage times at the barrier
358 were derived for power-law and periodic forcing time-dependent drift and
359 diffusion terms for the associated Fokker Planck equation using the method
360 of images. The general properties and limitations of this method were also
361 reviewed, with reference to previous results obtained in the field of neural
362 sciences and stochastic resonance. Particularly, we discussed how the ap-
363 plicability of the method of images to a Bm with time-dependent drift and
364 diffusion is limited to the case of a process with constant Péclet number, i.e.
365 with a time-independent ratio of drift and diffusion.

366 Where the time dependence is of the power-law type, the derived first
367 passage time density and survival functions share many analogies with the
368 statistics of inter arrival times between intermittent events when the con-
369 sidered system displays sporadic randomness. In the case of a periodic
370 time-dependence, first passage time statistics appear to be modulated by
371 the frequency of the forcing. The periodic forcing case has been also used to

372 show the approximate nature of solutions obtained by the method of images,
373 when time-dependent drift and diffusion terms are not linearly related. We
374 finally show how a Bm with power-law decaying drift and diffusion can be
375 used to describe the warm season dynamics of the total water equivalent in
376 mountainous regions.

377 **6. Acknowledgments**

378 This study was supported, in part, by the National Science Founda-
379 tion (nsf-ear 0628342, nsf-ear 0635787 and NSF-ATM-0724088), and the
380 Bi-national Agricultural Research and Development (BARD) Fund (IS-3861-
381 96). We wish to thank Adi Bulsara for the helpful suggestions. We also thank
382 Demetris Koutsoyiannis and the other three anonymous reviewers for their
383 helpful suggestions.

384 **References**

- 385 Abramowitz, M., & Stegun, I. A. (1964). *Handbook of Mathematical Func-*
386 *tions with Formulas, Graphs, and Mathematical Tables.* (ninth dover print-
387 ing, tenth gpo printing ed.). New York: Dover.
- 388 Adami, C. (1995). Self-organized criticality in living systems. *Phys. Lett. A*,
389 *203*, 29–32.
- 390 Bak, P., & Paczuski, M. (1995). Complexity, contingency, and criticality.
391 *PNAS*, *92*, 6689–6696.

- 392 Barnett, T., Malone, R., Pennell, W., Stammer, D., Semtner, B., & Wash-
393 ington, W. (2004). The effects of climate change on water resources in the
394 west: Introduction and overview. *Climatic Change*, *62*, 1–11.
- 395 Barnett, T. P., Adam, J. C., & Lettenmaier, D. P. (2005). Potential impacts
396 of a warming climate on water availability in snow-dominated regions.
397 *Nature*, *438*, 303–309.
- 398 Barnett, T. P., & Pierce, D. W. (2009). Sustainable water deliveries from
399 the colorado river in a changing climate. *P. Natl. Acad. Sci. Usa*, *106*,
400 7334–7338.
- 401 Barranguet, C., Kromkamp, J., & Peene, J. (1998). Factors controlling pri-
402 mary production and photosynthetic characteristics of intertidal microphy-
403 tobenthos. *Mar. Ecol-Prog. Ser.*, *173*, 117–126.
- 404 Bertness, M., & Leonard, G. (1997). The role of positive interactions in
405 communities: Lessons from intertidal habitats. *Ecology*, *78*, 1976–1989.
- 406 Bras, R. L. (1990). *Hydrology: An Introduction to Hydrological Science*.
407 Reading, MA: Addison-Wesley.
- 408 Bulsara, A. R., Lowen, S. B., & Rees, C. D. (1994). Cooperative behavior in
409 the periodically modulated wiener process: Noise-induced complexity in a
410 model neuron. *Phys. Rev. E*, *49*, 4989–5000.
- 411 Bulsara, A. R., Lowen, S. B., & Rees, C. D. (1995). Reply to “coherent
412 stochastic resonance in the presence of a field”. *Phys. Rev. E*, *52*, 5712–
413 5713.

- 414 Charles, H., & Dukes, J. S. (2009). Effects of warming and altered precipi-
415 tation on plant and nutrient dynamics of a new england salt marsh. *Ecol.*
416 *Appl.*, *19*, 1758–1773.
- 417 Cox, D. R., & Miller, H. D. (1965). *The Theory of Stochastic Processes*.
418 Boca Raton, Florida, USA: Chapman & Hall, CRC.
- 419 Daniels, H. (1982). Sequential tests constructed from images. *Ann. Stat.*,
420 *10*, 394–400.
- 421 De Walle, D., & Rango, A. (2008). *Principles of Snow Hydrology*. Cambridge,
422 UK: Cambridge university press.
- 423 Ehleringer, J., Cerling, T., & Helliker, B. (1997). C-4 photosynthesis, atmo-
424 spheric CO₂ and climate. *Oecologia*, *112*, 285–299.
- 425 Feller, W. (1971). *An Introduction to Probability Theory and Its Applications*,
426 *Vol. 2, 3rd Edition*. Wiley.
- 427 Gammaitoni, L., Hanggi, P., Jung, P., & Marchesoni, F. (1998). Stochastic
428 resonance. *Rev. Mod Phys.*, *70*, 223–287.
- 429 Gaspard, P., & Wang, X. (1988). Sporadicity - between periodic and chaotic
430 dynamical behaviors. *PNAS*, *85*, 4591–4595.
- 431 Hamlet, A., & Lettenmaier, D. (1999). Effects of climate change on hydrology
432 and water resources in the Columbia River basin. *J. Am. Water Resour.*
433 *As.*, *35*, 1597–1623.

- 434 Jensen, H. J. (1998). *Self-Organized Criticality : Emergent Complex Behavior*
435 *in Physical and Biological Systems (Cambridge Lecture Notes in Physics)*.
436 Cambridge, UK; New York, NY, USA: Cambridge University Press.
- 437 Johnson, N., Kotz, S., & Balakrishnan, N. (1994). *Continuous Univariate*
438 *Distributions* volume 1. New York, USA: Wiley and Sons.
- 439 Jung, P. (1993). Periodically driven stochastic-systems. *Phys. Rep.*, *234*,
440 175–295.
- 441 Kim, C., Talkner, P., Lee, E. K., & Haenggi, P. (2010). Rate description
442 of Fokker-Planck processes with time-periodic parameters. *Chem. Phys.*,
443 *370*, 277–289.
- 444 Lo, V., Roberts, G., & Daniels, H. (2002). Sequential tests constructed from
445 images. *Bernoulli*, *8*, 53–80.
- 446 Marks, D., Kimball, J., Tingey, D., & Link, T. (1998). The sensitivity of
447 snowmelt processes to climate conditions and forest cover during rain-on-
448 snow: a case study of the 1996 Pacific Northwest flood. *Hydrol. Proc.*, *12*,
449 1569–1587.
- 450 McClanahan, T., & Maina, J. (2003). Response of coral assemblages to the
451 interaction between natural temperature variation and rare warm-water
452 events. *Ecosystems*, *6*, 551–563.
- 453 McDonnell, M., Stocks, N., Pearce, C., & Abbott, D. (2008). *Stochastic*
454 *Resonance: From Suprathreshold Stochastic Resonance to Stochastic Signal*
455 *Quantization*. Cambridge, UK: Cambridge University Press.

- 456 Molini, A., Katul, G. G., & Porporato, A. (2009). Revisiting rainfall clus-
457 tering and intermittency across different climatic regimes. *Water Resour.*
458 *Res.*, *45*.
- 459 Pascual, M., Bouma, M., & Dobson, A. (2002). Cholera and climate: revis-
460 iting the quantitative evidence. *Microbes Infect.*, *4*, 237–245.
- 461 Patz, J., Campbell-Lendrum, D., Holloway, T., & Foley, J. (2005). Impact
462 of regional climate change on human health. *NATURE*, *438*, 310–317.
- 463 Pepin, N. C., & Lundquist, J. D. (2008). Temperature trends at high eleva-
464 tions: Patterns across the globe. *Geophys. Res. Lett.*, *35*.
- 465 Perona, P., D’Odorico, P., Porporato, A., & Ridolfi, L. (2001). Reconstruct-
466 ing the temporal dynamics of snow cover from observations. *Geophys. Res.*
467 *Lett.*, *28*, 2975–2978.
- 468 Polyanin, A. (2002). *Handbook of Linear Partial Differential Equations for*
469 *Engineers and Scientists*. New York, NY, USA: Chapman and Hall/CRC.
- 470 Redner, S. (2001). *A Guide to First Passage Processes*. Cambridge, UK:
471 Cambridge university Press.
- 472 Rigby, J. R., & Porporato, A. (2010). Precipitation, dynamical intermittency,
473 and sporadic randomness. *Adv. Water Resour.*, *33*, 923 – 932.
- 474 Rosenzweig, C., & Parry, M. (1994). Potential impact of climate-change on
475 world food supply. *Nature*, *367*, 133–138.
- 476 Schindler, M., Talkner, P., & Hanggi, P. (2005). Escape rates in periodically
477 driven markov processes. *Phys. A*, *351*, 40–50.

- 478 Talkner, P., Machura, L., Schindler, M., Hanggi, P., & Luczka, J. (2005).
479 Statistics of transition times, phase diffusion and synchronization in peri-
480 odically driven bistable systems. *New J. Phys.*, *7*.
- 481 You, Q. L., Kang, S. C., Pepin, N., Flugel, W. A., Yan, Y. P., Behrawan, H.,
482 & Huang, J. (2010). Relationship between temperature trend magnitude,
483 elevation and mean temperature in the tibetan plateau from homogenized
484 surface stations and reanalysis data. *Global Planet. Change*, *71*, 124–133.

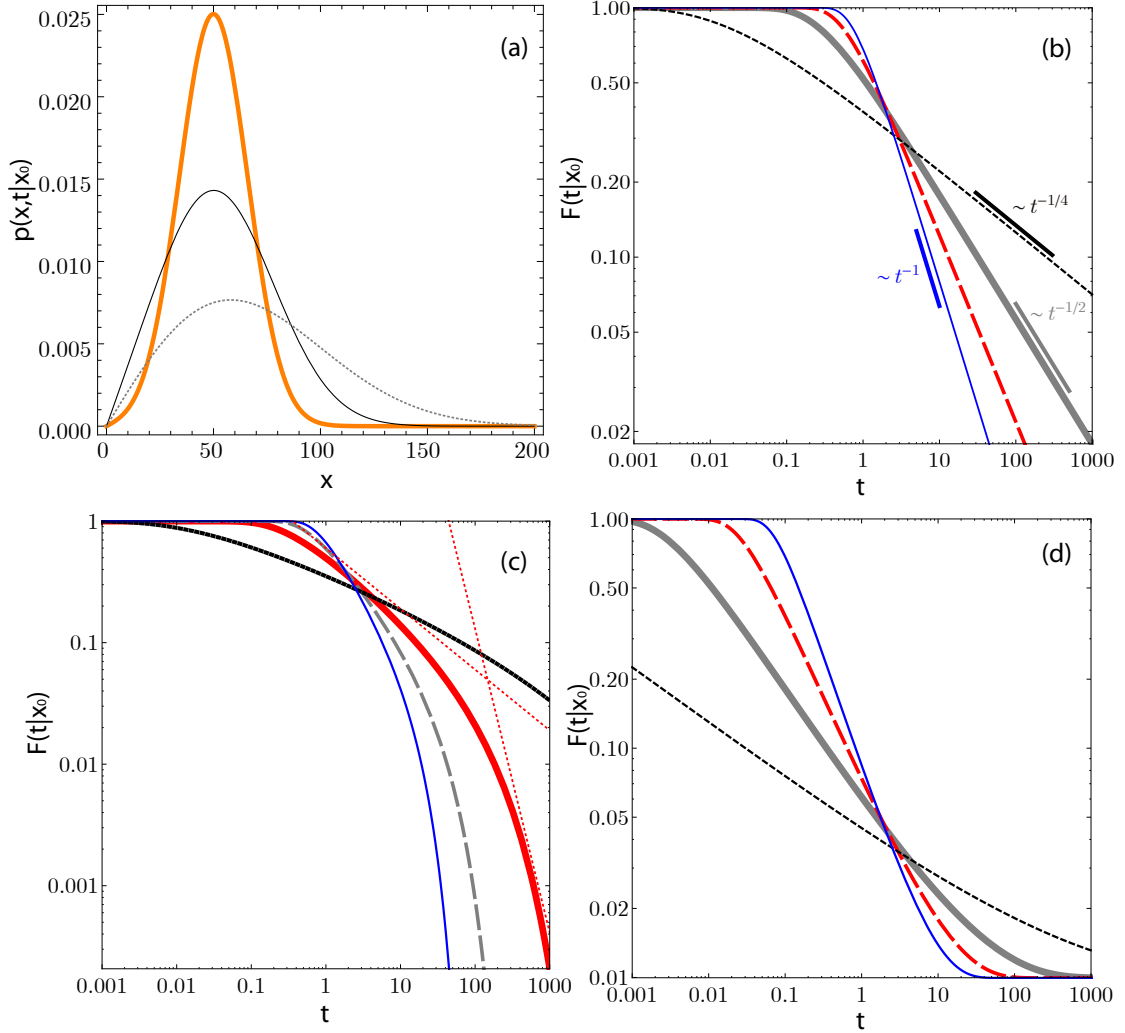


Figure 1: Conditional probability $p(x, t|x_0)$ at different fixed times t (a) and survival function $F(t|x_0)$ (b) for the pure power-law time dependent process described in Section 3.1, together with $F(t|x_0)$ for the negatively biased power-law process (c) and for the positively biased one (d). Panel (a) represents $p(x, t|x_0)$ at a fixed time $t = 15$ steps for $A = 15$, $x_0 = 50$, and $\alpha = -0.1$ (bold line), $\alpha = 0.5$ (thin line), and $\alpha = 1$ (dotted line). In (b) $F(t|x_0)$ is displayed as a function of t for $A = 1$, $x_0 = 1$ and $\alpha = 0$ (constant diffusion, bold line), $\alpha = -0.5$ (thin dotted line), $\alpha = 0.5$ (dashed line), and $\alpha = 1$ (thin line). Panels (c) and (d) display respectively a negatively biased power-law time dependent Bm and a positively biased one for the same set of parameters in (b) and $q = -0.1$ and $q = 0.1$.

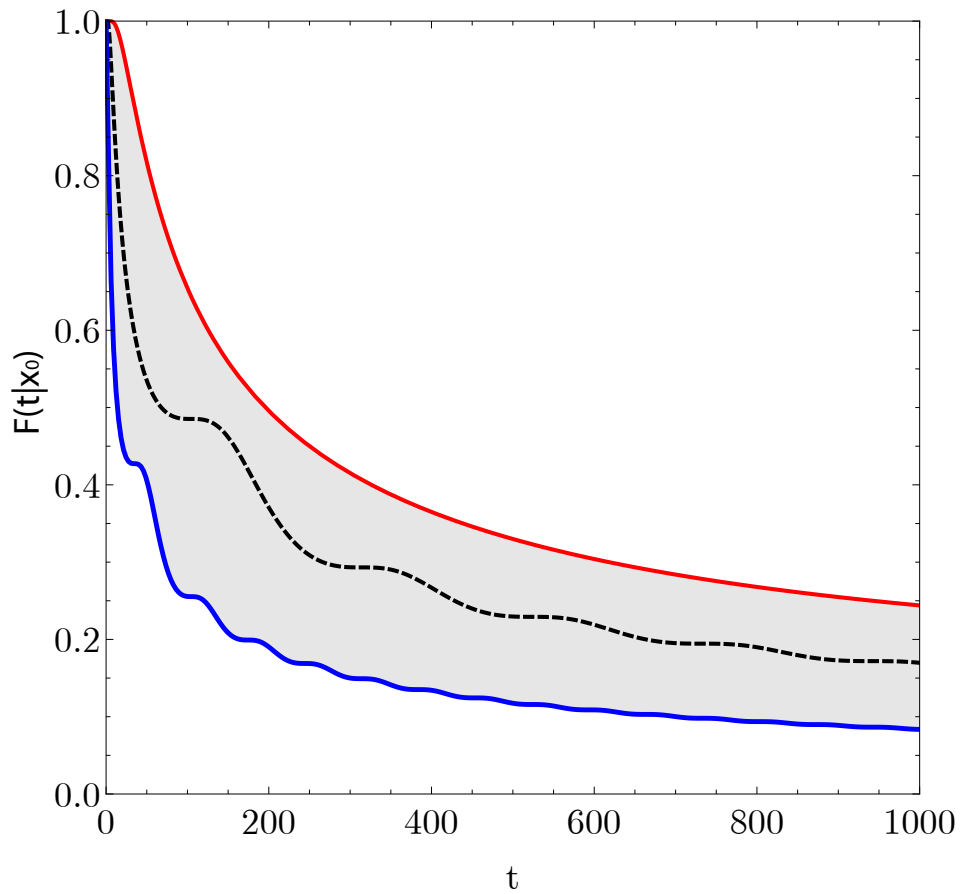


Figure 2: Survival function $F(t|x_0)$ for the periodic purely diffusive process described in Section 3.2 , and for $A = 15$ and $x_0 = 50$. Upper, dashed and lower curves represent F for $\omega = 0.0001$, $\omega = 0.015$, and $\omega = 0.045$, respectively.

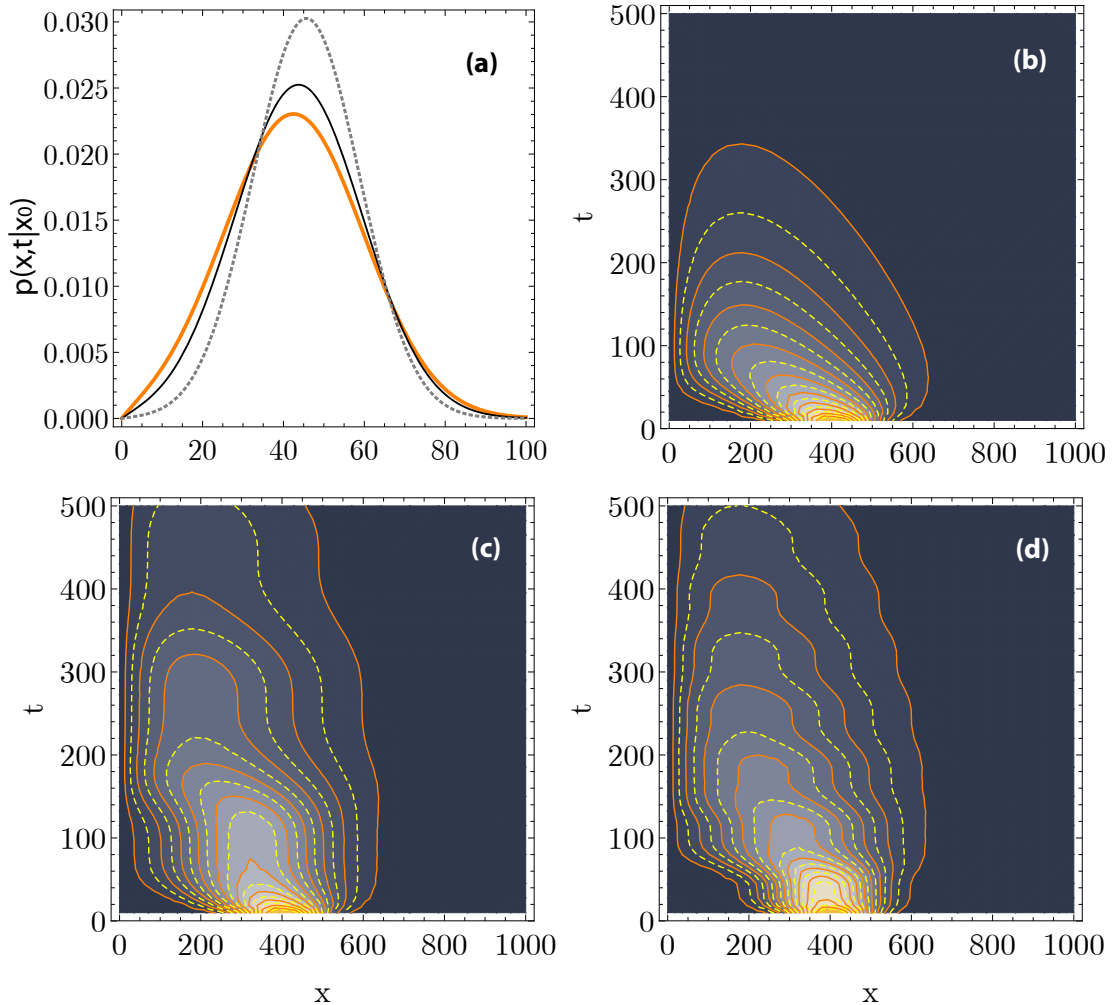


Figure 3: Conditional probability $p(x, t|x_0)$ for the periodic negatively biased Bm described in Section 3.2. Panel (a) represents $p(x, t|x_0)$ at a fixed time $t = 3$ steps for $A = 15$, $x_0 = 50$, $q = -0.05$, and $\omega = 0.0001$ (bold line), $= 0.5$ (thin line), and $= 0.9$ (dotted line). Also, contour plots (b) to (d) show $p(x, t|x_0)$ for $A = 15$, $x_0 = 450$ and $q = -0.01$ as a function of x and t , for $\omega = 0.0001$ (panel (b)), $\omega = 0.015$ (panel (c)), and $\omega = 0.045$ (panel (d)) respectively. Note how the negative drift forces the probability mass toward the barrier.

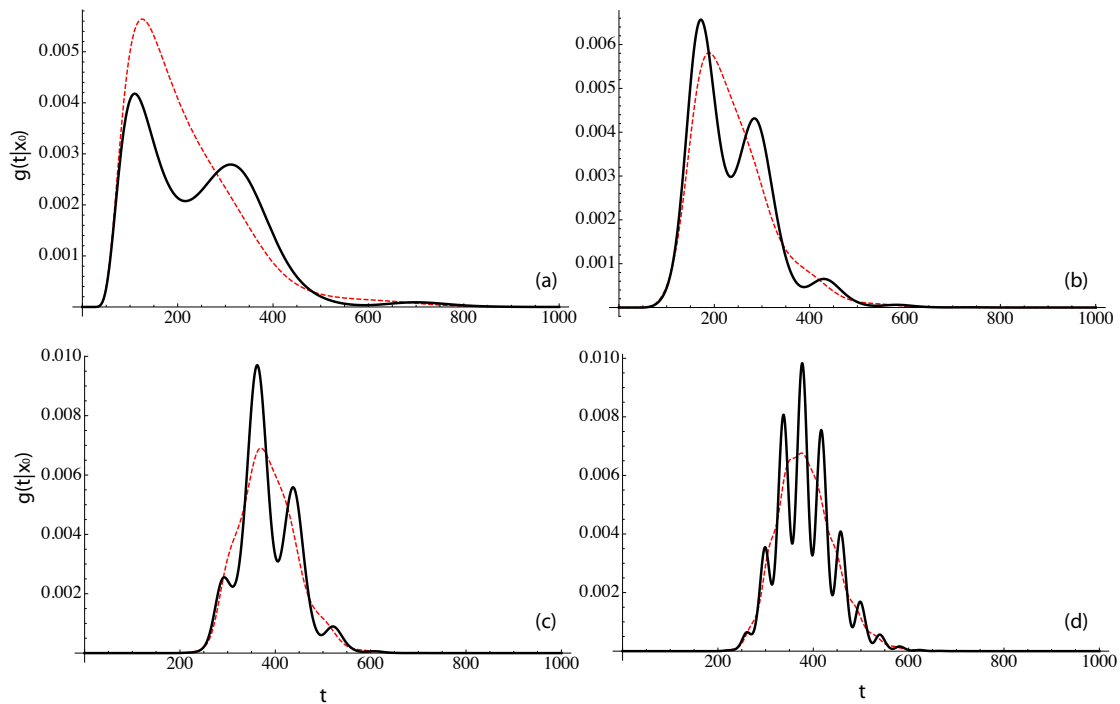


Figure 4: First passage densities $g(t|x_0)$ (bold black line, Eq. 44), and $\tilde{g}(t|x_0)$ (red dotted line, Eq. 45), respectively for (a) $\mu = 0.065$, $\sigma = 0.5$, $x_0 = 25$, $A = 0.032$ and $\omega = 0.016$; (b) $\mu = 0.065$, $\sigma = 0.35$, $x_0 = 15.5$, $A = 0.025$ and $\omega = 0.04$; (c) $\mu = 0.065$, $\sigma = 0.2$, $x_0 = 25$, $A = 0.03$ and $\omega = 0.07$, and (d) $\mu = 0.065$, $\sigma = 0.2$, $x_0 = 25$, $A = 0.03$ and $\omega = 0.15$. The discrepancy between $\tilde{g}(t|x_0)$ and $g(t|x_0)$ clearly signifies the failure of the method of images for problems with time-dependent Péclet numbers.

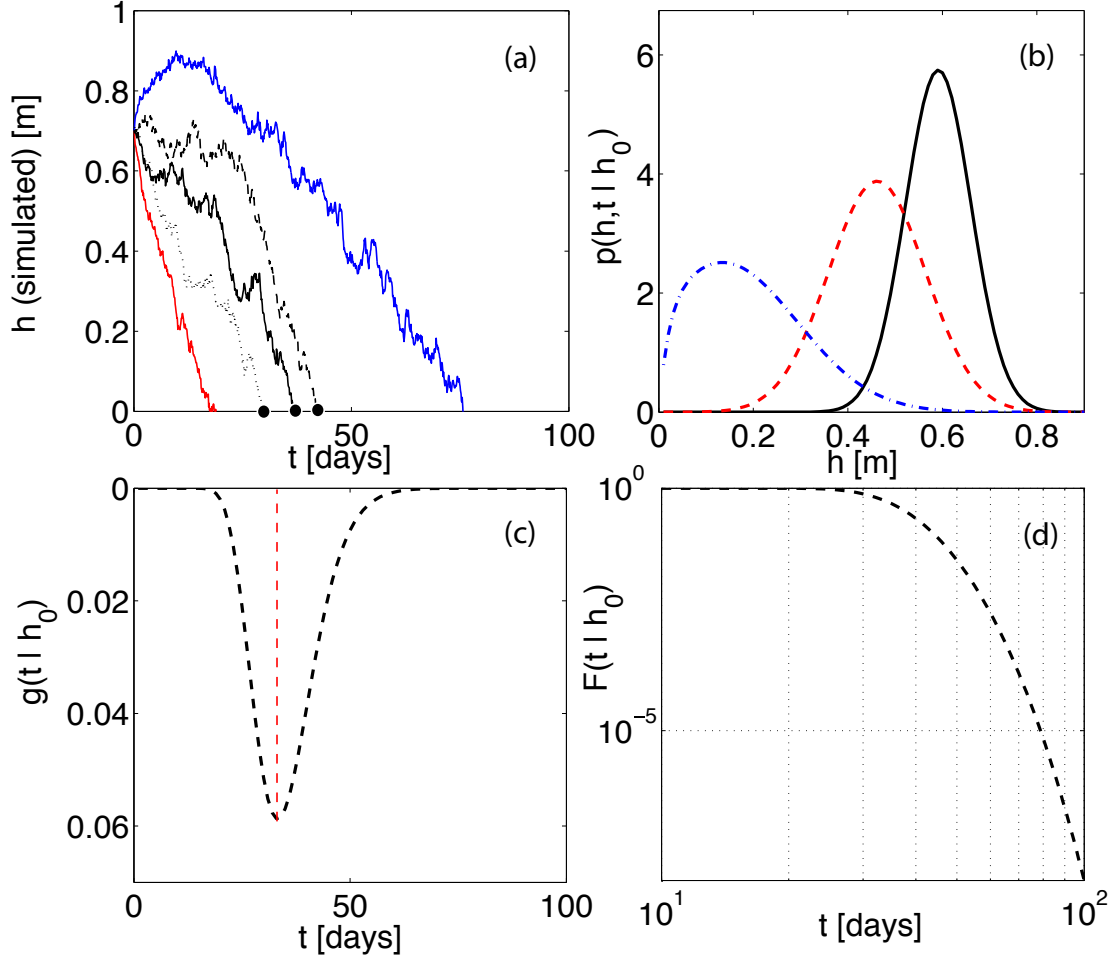


Figure 5: Sample trajectories of specific water equivalent from elevated regions during the melting season (a), and analytical results for the coupled stochastic melting-precipitation process of equation (46) (panels (b) to (d)). Numerical results were obtained by simulating Eq. (46) by means of an Euler algorithm with step 10^{-2} days. Panel (a) shows few sample trajectories of the process together with the curve of maximum values (upper curve) and minimum values (lower curve) over an ensemble of 10000 simulations, for $\alpha = 0.25$ and $k = 0.24 \text{ mm}^2/\text{days}^\alpha$. Analytical results for the conditional probability $p(h, t | h_0)$ at different instants, the first passage time density $g(t | h_0)$, and the survival function $F(t | h_0)$, are also shown in panels (b) to (d).